J Real-Time Image Proc
DOI 10.1007/s11554-010-0167-4

SPECIAL ISSUE

High-resolution, real-time 3D imaging with fringe analysis

Nikolaus Karpinsky · Song Zhang

Received: 28 March 2010 / Accepted: 5 July 2010

Abstract Real-time 3D imaging is becoming increasingly important in areas such as medical science, entertainment, homeland security, and manufacturing. Numerous 3D imaging techniques have been developed, but only a few of them have the potential to achieve realtime. Of these few, fringe analysis based techniques stand out, having many advantages over the rest. This paper will explain the principles behind fringe analysis based techniques, and will provide experimental results from systems using these techniques.

Keywords Real-time · 3D scanning · 3D imaging · Fringe analysis · Phase shifting

1 Introduction

With recent trends in entertainment moving towards 3D, such as James Camerons Avatar and Radioheads House of Cards [25], a need for 3D acquisition systems is growing. Science and engineering have also begun to realize the benefits of precise 3D measurement, yet are still looking for ways to acquire the 3D data. Over the years, numerous techniques have been developed to acquire 3D information, such as photogrammetry, shape from focus, shape from defocus, stereo vision, spacetime stereo, moiré, speckle, holography, time of flight, interferometry, fringe projection, and structured light. Advancements in the field have allowed some of these techniques to realize real-time capability, moving into a new classification of imaging known as real-time 3D imaging. In order to reach real-time 3D imaging, the 3D image acquisition, reconstruction, and display must all be realized simultaneously in real-time. Recent techniques that have been developed [3, 8, 26, 30] are based on different principals, yet rely on a common technique of using binary structured patterns. Although this binary structured pattern allows these techniques to reach real-time 3D imaging, they share the same caveat, the spatial resolution is limited to being larger than a single projector pixel [31]. For applications that require high spatial resolution this is not desirable, as the spatial resolution is limited by the projectors resolution.

To increase spatial resolution past the projectors resolution, a technique called fringe analysis may be implemented. Instead of using images with binary grayscale values, fringe analysis uses sinusoidally changing intensity values for the structured light being projected. Like binary structured patterns, more fringe images can be used to achieve higher accuracy, but this slows down the measurement speed. To reach real-time 3D imaging, a small number of fringe images (fringe patterns) are typically used. Under certain conditions, only a single fringe pattern is needed to reconstruct the 3D information, thus very high speed may be realized [28]. However, as the complexity of the geometries surface increases, the measurement accuracy is affected, requiring more fringe patterns. Complex 3D geometry requires a minimum number of three fringe images to reconstruct a single 3D shape [21]. Thus, developing a real-time 3D imaging system consists of weighing different tradeoffs, and tailoring the system to its intended application.

N. Karpinsky
Human Computer Interaction, Iowa State University, Ames, IA 50011, USA
e-mail: karpinsn@iastate.edu

S. Zhang (✉)
Mechanical Engineering Department, Human Computer Interaction, Iowa State University, Ames, IA 50011, USA
e-mail: song@iastate.edu

Published online: 06 August 2010

Throughout our research, we have developed various real-time 3D imaging systems, tailoring each to a specific purpose. By using three fringe images, we developed a real-time 3D imaging system that can acquire 3D geometry at 40 frames/s [32] with a image resolution of 532 × 500. Another system we developed measures absolute 3D geometry at 60 frames/s [35] by using a modified 2 + 1 phase-shifting algorithm [37] with an image resolution of 640 × 480. Real-time 3D geometry acquisition, reconstruction, and display has also been reached by using a multilevel quality guided phase-unwrapping algorithm [39] and adopting the parallel processing power of a GPU [38].

We have explained various techniques to reach real-time 3D imaging based on digital fringe projection techniques in the previous paper by Zhang [31]. Specifically, that paper has focused on the real-time 3D shape measurement techniques based on phase-shifting methods. However, phase-shifting based methods are only a small group of fringe analysis techniques for 3D shape measurement. In this paper, we will explain the principal behind the fringe analysis technique, summarize recent advances that use the technique, and then will present some experimental results to show the advantages and shortcomings of each technique. Since digital video projectors allow for a higher degree of flexibility over other methods, our implementations focus on producing the sinusoidal fringe patterns with a digital projector. This technique is called digital fringe projection. Although the projection method has certain unique characteristics, similar analysis approaches can be applied to fringe images generated by other techniques.

Because of the nature of generating sinusoidal fringe patterns by a digital-light-processing (DLP) projector, it is difficult for such a system to realize real-time 3D shape measurement without any modifications. In addition, the fringe projection speed is fundamentally limited to a relatively slow rate (typically 120 Hz) because it requires 8 bits to generate sinusoidal fringe patterns. To circumvent these problems, new fringe generation means need to be used. In this paper, we will also discuss a recently developed fringe generation technique that generates sinusoidal fringe patterns by defocusing binary structured patterns.

2 Digital fringe projection system

Figure 1 shows a typical digital fringe projection system. A computer generates a digital fringe pattern consisting of vertical stripes that are sent to a digital video projector. The projector projects the fringe images onto the object, and the objects geometry deforms the fringe images as the vertical stripes bend around the contour of the object. At this point, the camera captures the distorted fringe image, and sends it to the computer for analysis. The computer analyzes the fringe image using triangulation with point correspondence, obtaining the 3D information. Since the fringe pattern is sinusoidal, each vertical straight line corresponds to one phase value in the frequency domain. The phase value is used for 3D reconstruction because the intensity value is very sensitive to the surface reflectivity variations. Finally, using fringe analysis the phase can be retrieved from the fringe images. The next few sections will introduce different approaches for phase retrieval.

3 Real-time 3D imaging using a single fringe image

If a single image is sufficient to perform 3D shape measurement, the 3D imaging speed can then be as fast as the image acquisition speed. This is the optimal case for real-time 3D imaging, as 3D reconstruction can match the camera's image acquisition speed. The technique of using a single fringe image to obtain the phase is called the Fourier method, which has been proposed by Takeda and Mutoh [29]. In this section, we will introduce a 3D shape recovery technique using a single fringe image.

3.1 Principle

In general, a typical fringe image can be written as

$$I(x,y) = I'(x,y) + I''(x,y)\cos[\phi(x,y)]. \quad (1)$$

Here $I'(x, y)$ is the average intensity or the DC component, $I''(x, y)$ is the intensity modulation, and $\phi(x, y)$ is the phase to be solved for.

Equation (1) can be re-written as

$$I(x,y) = I'(x,y) + I''(x,y)\left[e^{j\phi(x,y)} + e^{-j\phi(x,y)}\right]/2. \quad (2)$$

In this equation, $e^{-j\phi(x,y)}$ is the conjugate of $e^{j\phi(x,y)}$. If a Fourier transform is applied, and the DC and the conjugate

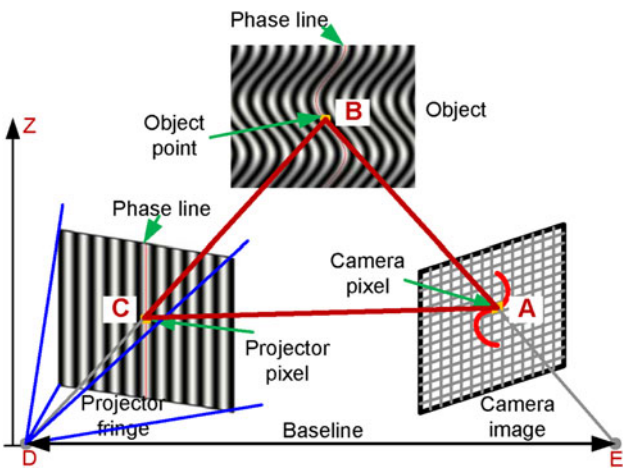

Fig. 1 Typical setup of a digital fringe projection

components are filtered out, the recovered signal by an inverse Fourier transform will give

$$\tilde{I}(x,y) = I''(x,y)e^{j\phi(x,y)}/2. \quad (3)$$

From Eq. (3), the phase can be solved for by

$$\phi(x,y) = \tan^{-1}\left\{\frac{Im[\tilde{I}(x,y)]}{Re[\tilde{I}(x,y)]}\right\}. \quad (4)$$

Here $Im(x)$ denotes the imagery part of a complex variable x, while $Re(x)$ denotes the real part of x. The phase value ranges from $-\pi$ to $+\pi$ with 2π modus due to the arctangent. The phase map is also called the wrapped phase map. To obtain a continuous phase map, an additional step called phase unwrapping needs to be applied. The phase unwrapping step is essentially finding the 2π jumps from neighboring pixels, and removing them by adding or subtracting an integer number of 2π to the corresponding point [6]. The 3D coordinates can then be reconstructed using the unwrapped phase, assuming that the system is properly calibrated [33].

3.2 Experimental results

To illustrate how this technique works, we captured a single fringe image using a 3D imaging system we developed. Figure 2a shows a typical fringe image captured by the camera. Figure 2b shows the image after applying the fast Fourier transform (FFT). There are two conjugate frequency components and the average.

If only a single frequency component is selected, as shown in the window, the phase can be calculated from the complex image obtained from inverse Fourier transform of the selected frequency, as shown in Fig. 2c. Figure 2d shows the unwrapped phase map. The unwrapped phase map can then be converted to 3D coordinates based on the calibration of the system.

Since only one fringe image is used to obtain a 3D shape, this technique works nicely for fast motion applications. An example of such an application is measuring vibration. Figure 3 shows some frames of a vibrating cantilever beam; the fringe images are captured at 2,000 fps with an exposure time of 0.5 ms. This experiment demonstrates that the 3D profiles can be captured efficiently by this technique. This technique can also be used to measure other dynamic shapes, as surveyed in this paper [28].

However, as illustrated in all these examples the measured surface is very smooth and uniform. This is a typical requirement for a single fringe image based real-time 3D imaging system. This is because the single fringe technique requires the frequency of the projected fringe to be much higher than the surface geometry changes. Even with such a shortcoming, this technique is still very useful when the measurement surface meets this requirement.

4 Real-time 3D imaging using two fringe images

As can be seen from the previous section, a single fringe image can be used to recover a 3D shape. However, in order to obtain the phase in the frequency domain, the DC component must be filtered out. For a uniform fringe image with approximately uniform surface reflectivity, the DC frequency only covers a very small area, thus can be easily

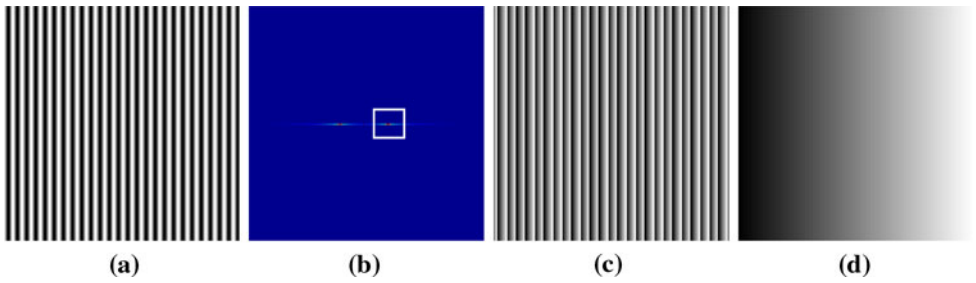

Fig. 2 Experimental result of using a single fringe images for 3D shape measurement. **a** Fringe image, **b** Fourier spectrum of the fringe image, **c** the phase map filtering the desired frequency signal, **d** unwrapped phase map

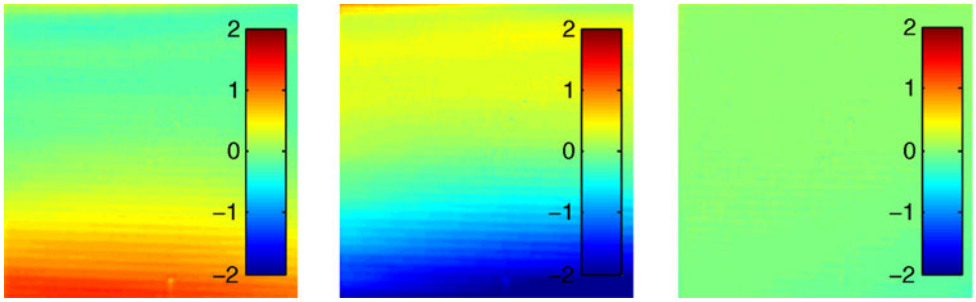

Fig. 3 Typical measurement frames of a vibration cantilever bar. The data is captured at 2,000 fps with an exposure time of 0.5 ms

filtered out. However, if the surface reflectivity varies significantly across the surface, it would be challenging to separate the DC component and the desired frequency. To alleviate this problem, Guo and Huang [9] introduced a technique that uses two fringe images.

4.1 Principle

The principle of this technique is similar to the previously introduced method except it requires the capturing of an additional image

$$I_a(x, y) = I'(x, y). \tag{5}$$

Before applying the Fourier transform, the fringe image is obtained by taking the difference between the images.

$$I_m(x, y) = I(x, y) - I_a(x, y) = I''(x, y)\cos[\phi(x, y)]. \tag{6}$$

By doing this, the DC component will not affect the measurement significantly, thus the measurement quality can be improved. However, it sacrifices measurement speed as two fringe images must be captured to construct a 3D shape.

4.2 Experimental results

To verify the performance of this technique, we compared it to the single fringe technique, measuring a sculpture with non uniform surface reflectivity as shown in Fig. 4a. The captured fringe is shown in Fig. 4b. The figure clearly shows that the fringe intensity varies from point to point. Figure 4c shows the phase map, and Fig. 4d shows the zoom in view of the phase map. There are significant artifacts in the phase map which will cause measurement error. The unwrapped phase map is shown in Fig. 4e, and the reconstructed 3D shape is shown in Fig. 4f. This experiment shows that if the surface is complex, a single fringe image cannot produce high quality 3D measurement.

If the average image $I_a(x, y)$ (shown in Fig. 5a) is captured and subtracted from the fringe image (as shown in Fig. 4b), the phase map can be obtained with higher measurement quality. Figure 5b shows the zoom-in view of the phase image, clearly showing the improvement of the phase map. Thus the 3D measurement will be significantly enhanced. Figure 5c shows the 3D shape. By using two fringe images, the influence of surface reflectivity variations is significantly

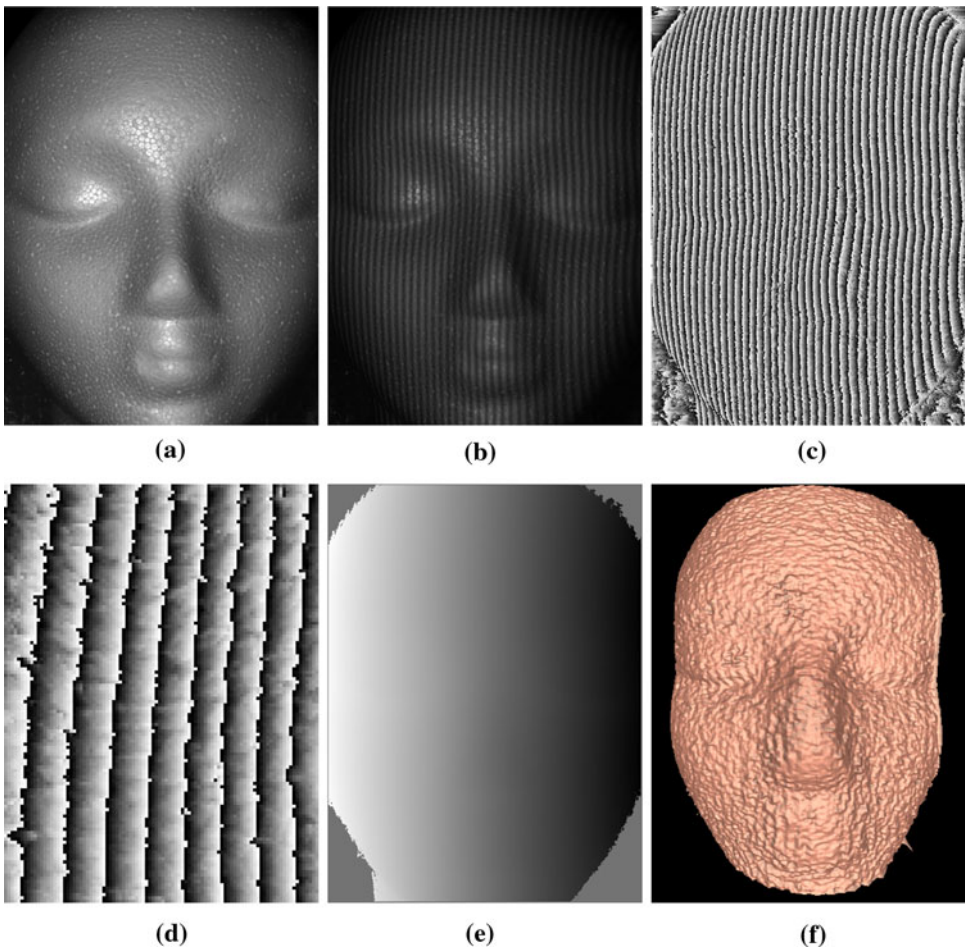

Fig. 4 More complex 3D surface measurement result using a single fringe image. **a** Photograph of the object to be measured, **b** Fringe image, **c** Wrapped phase map, **d** zoom-in view of the unwrapped phase map, **e** unwrapped phase map, **f** 3D reconstructed shape rendered in shaded mode

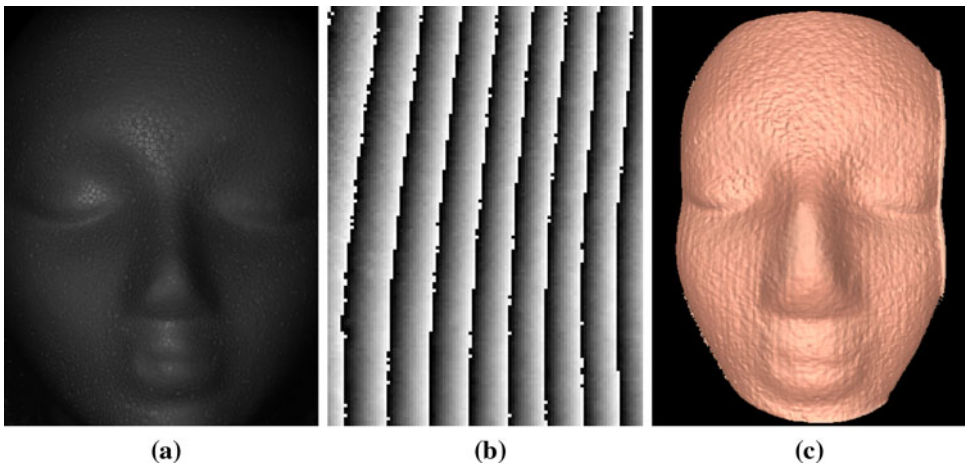

Fig. 5 More complex 3D shape using two fringe images. **a** The average image $I_a(x, y)$, **b** zoom in view of the phase map, **c** 3D reconstructed result

reduced, thus improving the measurement quality. With this technique, a lot more detail can be recovered.

Even though the measurement quality is significantly improved, it is still very difficult for this technique to measure complex 3D surfaces because of its fundamental limitation: surface changes must be slower than the fringe changes. This is because the phase cannot be solved for explicitly from the fringe image point by point. If the phase can be solved for each individual point, the surface structure requirement can be eliminated since it would not rely on the neighboring pixel information to retrieve the phase. Equation (1) shows that there are three unknowns in the equation $I'(x, y)$, $I''(x, y)$, and $\phi(x, y)$. Therefore, if another image is provided, the phase $\phi(x, y)$ can be uniquely solved. This is where the requirement for three fringe images for a single 3D shape measurement comes from.

5 Real-time 3D imaging using three fringe images

From three fringe images the phase can be uniquely solved for, thus it allows for the measurement of complex 3D shapes. In this section, we will introduce a real-time 3D imaging system based on this technique.

5.1 Principle

5.1.1 Three-step phase-shifting algorithm

The previously introduced methods depended on obtaining the phase from Fourier analysis. If three fringe images are available, the phase can be uniquely solved. Among these multiple fringe analysis techniques, the technique based on phase-shifting has been widely adopted in optical metrology [21]. In this technique, the fringe is shifted spatially from frame to frame with a known phase shift. By analyzing a set of phase-shifted fringe images, the phase can be obtained. The phase-shifting based techniques have the following advantages: (1) high measurement speed, because it only requires three fringe images to recover one 3D shape; (2) high spatial resolution, because the phase can be obtained pixel by pixel, thus the measurement can be performed pixel by pixel; (3) less sensitivity to surface reflectivity variations, since the calculation of the phase will automatically cancel out the DC components.

Over the years, a number of phase-shifting techniques have been developed, including three-step, four-step, double three-step phase shifting and others [21]. For real-time 3D imaging, using the minimum number of fringe images is desirable, thus a three-step phase-shifting algorithm is usually used. For a three-step phase-shifting algorithm, if the phase shift is $2\pi/3$, the three required phase-shifted fringe images can be written as

$$I_1(x,y) = I'(x,y) + I''(x,y)\cos[\phi(x,y) - 2\pi/3], \tag{7}$$

$$I_2(x,y) = I'(x,y) + I''(x,y)\cos[\phi(x,y)], \tag{8}$$

$$I_3(x,y) = I'(x,y) + I''(x,y)\cos[\phi(x,y) + 2\pi/3]. \tag{9}$$

Solving Eqs. (7)–(9) simultaneously, we obtain the average intensity

$$I'(x,y) = (I_1 + I_2 + I_3)/3, \tag{10}$$

the intensity modulation

$$I''(x,y) = \frac{\sqrt{3(I_1 - I_3)^2 + (2I_2 - I_1 - I_3)^2}}{3}, \tag{11}$$

the phase

$$\phi(x,y) = \tan^{-1}\left[\frac{\sqrt{3}(I_1 - I_3)}{2I_2 - I_1 - I_3}\right]. \tag{12}$$

From the same equations, we can also obtain the texture image, $I_t(x, y) = I'(x, y) + I''(x, y)$, and the data modulation

$$\gamma(x,y) = \frac{I''}{I'} = \frac{\sqrt{3(I_1 - I_3)^2 + (2I_2 - I_1 - I_3)^2}}{I_1 + I_2 + I_3}. \quad (13)$$

The data modulation indicates the fringe quality, with 1 being the best. Data modulation is often valuable for phase unwrapping where the progress path is vital [6]. A measurement example using the three fringe images is shown in Fig. 6. It clearly shows that the measurement quality is much better than that of a two fringe image or a single fringe image based technique.

5.1.2 Real-time 3D image acquisition

Since only three fringe images are used, they can be encoded as the three primary color channels (red, green and blue, or RGB) and projected at once [5, 13, 24]. However, the measured quality is affected to a various degree if the measured surface has strong color variations. In addition, the color coupling between RG and GB also affect the measurement quality if no filtering is used [24].

The problems induced by using color fringe patterns can be eliminated if three monochromatic fringe patterns are rapidly projected sequentially. The unique projection mechanism of a single-chip digital-light-processing (DLP) projection system makes this rapid switching feasible, thus real-time 3D imaging can be realized. Figure 7 shows the layout of such a system. Three phase-shifted fringe images are encoded as the RGB channels of the projector. The color fringe image is then projected by the projector channel by channel sequentially. If the color filters of the DLP projector are removed, the color images will be be projected in monochromatic mode, thus the problems related to color are not present. A high-speed CCD camera, synchronized with the projector is used to capture the three channel images one by one. By applying the three-step phase-shifting algorithm to three fringe images, the phase and thus the 3D shape can be obtained. By this means, we have reached 3D data acquisition at 40 fps [32], and later on achieved 60 fps [37].

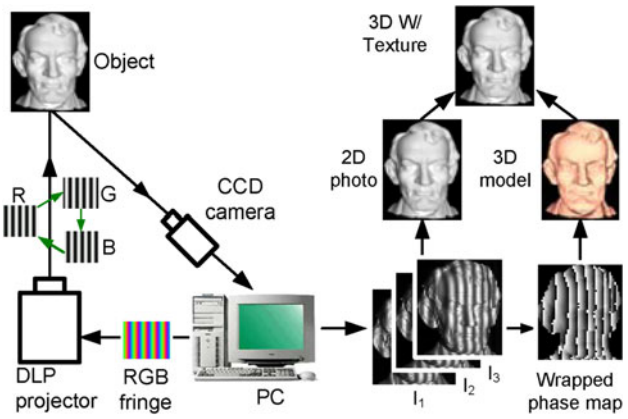

Fig. 7 The layout of the real-time 3D imaging system we developed

5.1.3 Real-time 3D reconstruction and visualization

In order to realize real-time 3D imaging, the phase wrapping and unwrapping speed must be realized in real-time. We have developed a fast three-step phase-shifting algorithm to improve the phase wrapping speed by about 3.4 times [12]. This algorithm essentially approximates the arctangent function with an intensity ratio calculation in the same manner as that of the trapezoidal phase-shifting algorithm [15]. The approximation error is then compensated for by a small look-up-table (LUT).

The phase unwrapping obtains the smooth phase map by removing the 2π discontinuities. Over the years, numerous robust phase unwrapping algorithms have been developed that include the branch-cut algorithms [17, 27], the discontinuity minimization algorithm [4], the L^p-norm algorithm [7], the region growing algorithm [1, 16], the agglomerative clustering-based approach [22], and the

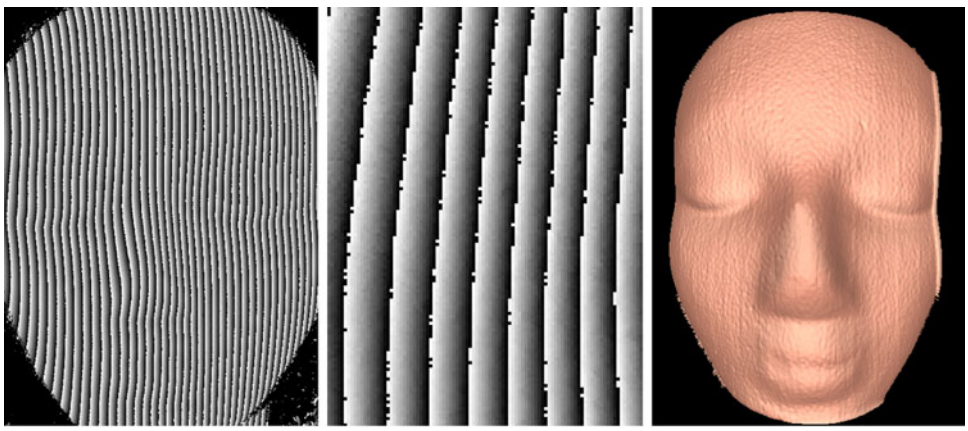

Fig. 6 More complex 3D shape using three fringe images. **a** The phase map, **b** zoom in view of the phase map, **c** 3D reconstructed result

least-squares algorithms [2]. However, a conventional robust phase unwrapping is usually very slow for real-time processing: it takes anywhere from a few seconds, to a few minutes, to even a few hours to process a standard 640 × 480 phase map [6]. There are some rapid but not robust phase unwrapping algorithms, such as the flood filling and the scan line algorithms [32, 39]. However, these algorithms are usually very sensitive to the noise of the phase map.

By combining the advantages of the the rapid scan line phase shifting algorithm and a robust quality guided phase-shifting algorithm, we developed a real-time phase unwrapping algorithm [39]. In particular, the phase map is evaluated and quantified into different quality levels using multiple thresholds: the unwrapping process starts with the highest quality level points using the scan line algorithm and then moves to the lower quality ones. The quality map is calculated based on phase gradient, high-quality data means low gradient of the points.

The scan-line algorithm is as follows. The process starts from one good point near the center of the image. After images are divided into four patches by the horizontal and vertical lines through the start point, each patch is unwrapped by the scanline method. In this scan-line method, one horizontal scan-line scans from the start point to the image border. Then the scan-line advances vertically from the start point to the image border to scan another row. The neighbors of one scanned point can be divided into two groups: the neighbors that faced the start point and the neighbors that faced the border. If at least one of its neighbors that faced the start point is unwrapped, a point will be unwrapped and marked as unwrapped. This point with no unwrapped neighbor facing the start point, but with at least one valid neighbor facing the border, will be pushed to the stack. After all points in a patch are scanned, the points in the stack will be popped one by one in reverse order. The popped point with at least one unwrapped neighbor facing the border will be unwrapped, while other points are abandoned. The merit of this method is that each point is scanned only once while it has two chances to be unwrapped. Therefore it results in better unwrapping results. Experiments demonstrated that for a 640 × 480 phase map, it only takes approximately 18.3 ms for the whole unwrapping process.

With this method, the lower quality points will not propagate and drastically affect the high quality points. This algorithm is a tradeoff between robustness and speed. We are mostly interested in human facial expression measurement, and for this application this algorithm works reasonably well. Figure 8 shows a typical measurement result of human facial expressions. It should be noted that because of the facial hair, the surface reflectivity

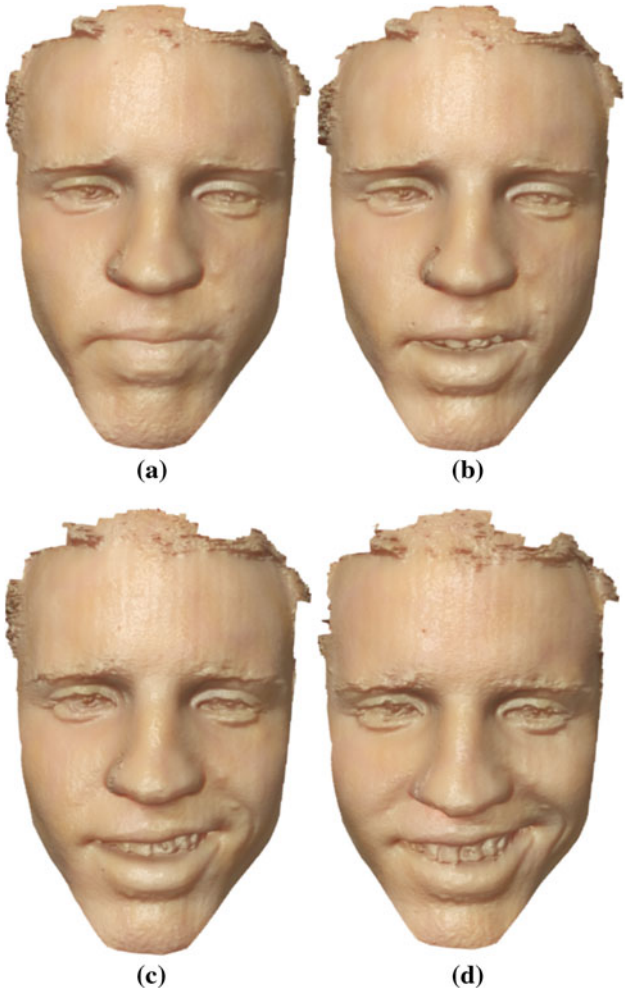

Fig. 8 Facial shape measurement. **a** Subject in neutral state, **b–d** expression on subjects face evolving through time into a smiling state. The data is captured at 60 fps with a resolution of 640 × 480

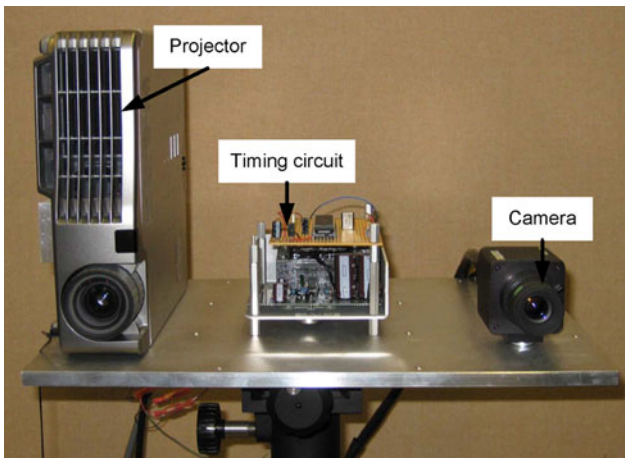

Fig. 9 The photograph of the real-time 3D imaging system

variations are large, and the phase unwrapping is usually very challenging, but our algorithm can unwrap the phase correctly for most cases.

To reach real-time 3D imaging, the phase map has to be converted to 3D coordinates and visualized in real-time. We found that it is very challenging to accomplish these tasks by central processing units (CPUs). Because the phase-to-coordinate conversion consists of simple point by point matrix operations, it can be efficiently calculated in parallel on a graphics processing unit (GPU). Because the input data is just the phase value at each point instead of computed 3D coordinates, data transfer from the CPU to the GPU is drastically reduced. In addition, because the coordinates are computed on GPU, they can be rendered immediately without accessing CPU data. By adopting this technique, real-time 3D imaging has been accomplished by using a three-step phase-shifting algorithm [38].

5.2 Experimental results

Figure 9 shows the developed hardware system. The whole size of the system is approximately $15'' \times 12'' \times 14''$. The system uses a high-speed CCD camera (Pulnix TM-6740 CL), with a maximum frame rate of 200 fps. The sensor pixel size is H: 7.4 μm and V: 7.4 μm. The maximum data speed for this camera is 200 frames per second. The camera resolution is 640 × 480, and the lens used is a Fujinon HF16HA-1B f = 16 mm lens. The projector (PLUS U5-632h) has an image resolution of 1024 × 768, and a focal length of $f = 18.4$–22.1 mm. This projector refreshes at 120 Hz, thus, this system can theoretically reach 120 Hz 3D imaging speed. However, due to the speed limit of the camera, we can only capture fringe images at 180 fps. Since three fringe images are needed to reconstruct one 3D shape, the 3D imaging speed is actually 60 Hz.

High quality natural facial expressions can be captured since the measurement speed is so fast. Figure 10 shows frames from the forming of a human facial expression. It clearly indicated that the details of the facial expression are captured fairly well. It should be noted that the data was processed with a 7 × 7 Gaussian smoothing filter to reduce the most significant random noise.

As introduced earlier, we are not only able to acquire 3D shape in real-time, but also are able to simultaneously process and display them at high speed. Figure 11 shows an experimental result of measuring a human face. The right figure shows the real subject, and the left shows the 3D geometry acquired and rendered on the computer screen at the same time. The simultaneous 3D data acquisition, reconstruction, and display speed achieved is 30 frames/s.

6 New fringe generation technique

Conventionally, fringe images are either generated by laser interference, or by a fringe projection technique. A fringe projection technique is broadly used because of its flexibility in generating sinusoidal fringe patterns. However, it usually requires at least 8-bit grayscale values to represent a high-quality fringe image. Because of the complexity of a fringe projection system, it usually has the following shortcomings:

– *Projector nonlinearity problem*. Because the projector is a nonlinear device, generation of sinusoidal fringe images is difficult. Different algorithms have been proposed to calibrate and correct the nonlinearity of the projector [10, 14, 18, 23, 34, 36], but it remains difficult to accurately represent the nonlinear curve. To some extent, the nonlinearity of the system is also caused by the graphics card that connects with the projector. We

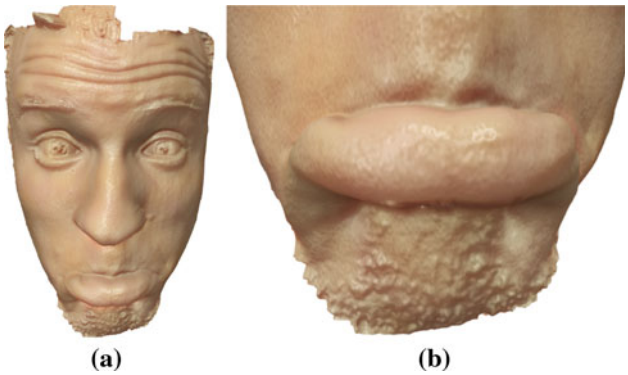

Fig. 10 Facial shape measurement. **a** 3D facial data rendered in shaded mode, **b** zoom-in view of the mouth region. The data are captured at 60 fps with a resolution of 640 × 480

Fig. 11 Simultaneous 3D data acquisition, reconstruction, and display. The system achieved a real-time 3D imaging at a frame rate of 30 fps with an image resolution of 640 × 480 per frame

found that the nonlinearity of the projector needs to be re-calibrated if a different video card is used. We also found that the projector's nonlinearity actually changes over time, thus frequent calibration is needed for high quality measurement. This is certainly not desirable because the nonlinearity calibration is usually a time consuming procedure.

– *Synchronization problem*. Since a DLP projector is a digital device, and it generates images by time integration [11], the synchronization between the projector and the camera is vital. Any mismatch will results in significant measurement error [20].
– *Minimum exposure time limitation*. Because the projector and the camera must be precisely synchronized, the minimum exposure time used for each fringe image capture is actually limited by the projector's refresh rate, typically 120 Hz. Thus, the minimum exposure time to use is actually 2.78 ms. However, when capturing fast motion, a shorter exposure time is usually required. This technique limits potential fast motion capture applications.

All these above mentioned issues are introduced by the conventional fringe generation technique, i.e., using 8-bit grayscale images. If a new fringe generation mechanism is employed that only requires 1-bit images, all these problems can be either avoided or significantly reduced. This is the motivation to explore this potential possibility.

6.1 Principle of fringe pattern generation using defocusing

We recently found that by defocusing binary structured patterns, sinusoidal fringe patterns can be generated [19]. This is based on our two observations: (1) seemingly sinusoidal fringe patterns often appear on the ground when the light shines through an open window blinds; (2) the sharp features of an object are blended together in a blurring image that is captured by an out-of-focus camera. The former gives the insight that an ideal sinusoidal fringe pattern could be produced from a binary structured pattern; the latter provides the hint that if the projector is defocused, the binary structured pattern might become an ideal sinusoidal one.

Figure 12 illustrates how to generate sinusoidal fringe patterns by using defocusing. If the projector is defocused

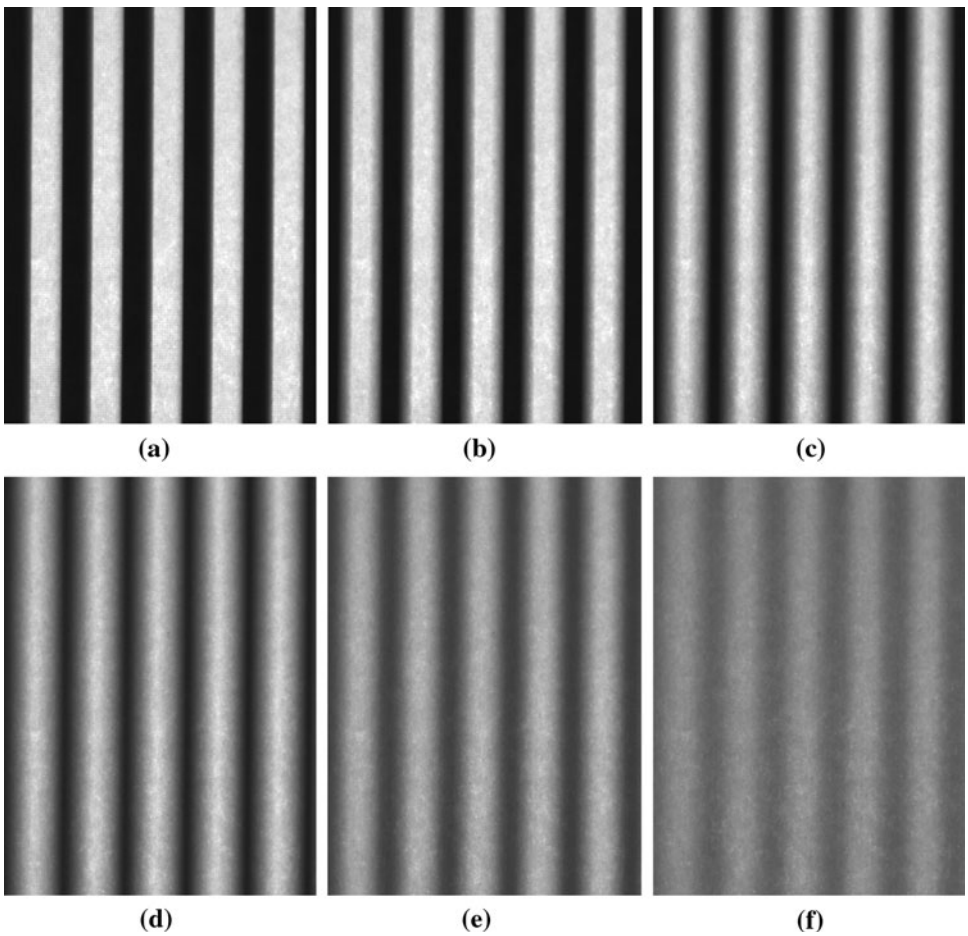

Fig. 12 Example of sinusoidal fringe generation by defocusing a binary structured patterns. **a**–**f** shows when the projector is defocused at different degrees, **a** the projector is in focus, while **f** shows that when the projector are defocused too much

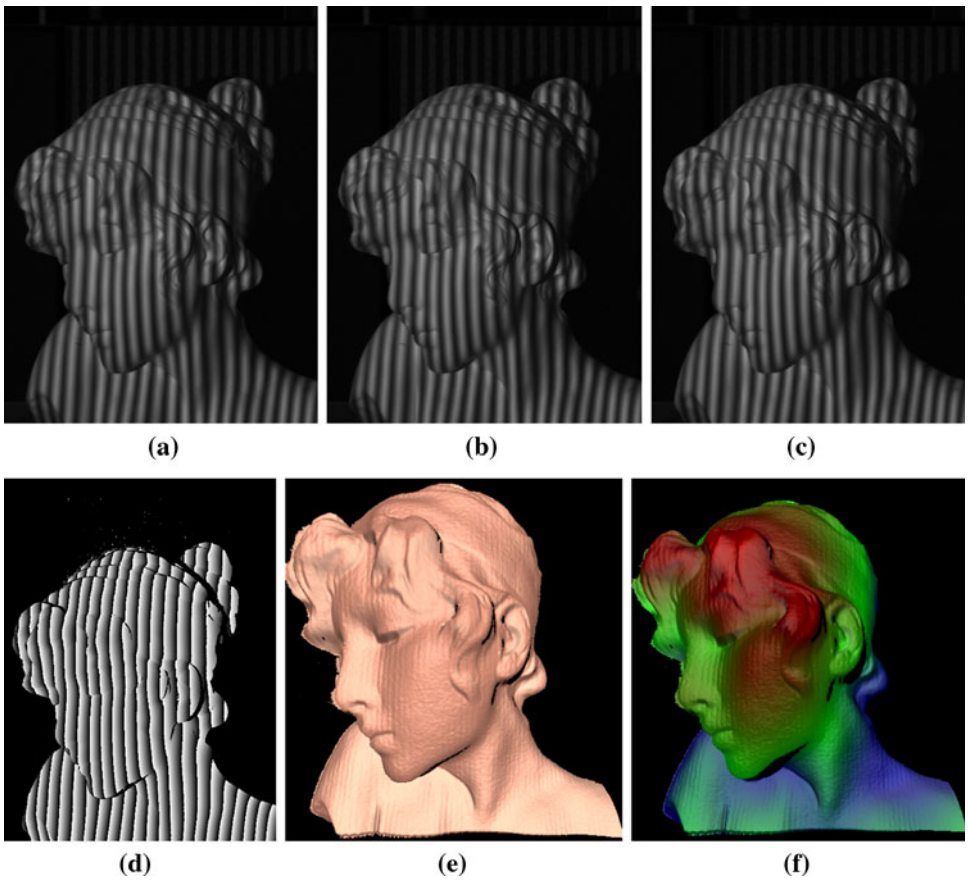

Fig. 13 Example of sinusoidal fringe generation by defocusing a binary structured patterns. **a** $I_1(-2\pi/3)$k, **b** $I_2(0)$, **c** $I_3(2\pi/3)$, **d** wrapped phase map, **e** 3D reconstructed result, **f** 3D shape with color encoded depth map

to different degrees, the binary structured patterns are deformed differently. When the projector and the camera are in focus, the fringe patterns have very obvious binary structures, as shown in Fig. 12a. With the increase of the defocusing degree, the binary structures are less and less clear, and they become more and more sinusoidal. However, if the defocusing degree is too much the sinusoidal structure becomes obscure, as indicated in Fig. 12f. It should be noted that during all experiments, the camera is always in focus.

This technique has the following advantages compared with the conventional fringe generation techniques [20]:

1. There is no need to calibrate the nonlinear gamma of the projector because only two intensity levels are used;
2. It is very easy to generate sinusoidal fringe patterns because no complicated algorithms are necessary;
3. There is no need to precisely synchronize the projector with the camera, and
4. The measurement is less sensitive to exposure time used. Therefore, the defocused binary pattern method is advantageous for 3D shape measurement using a commercial DLP projector.

6.2 Experimental results

This technique has been verified by measuring a complex sculpture, as shown in Fig. 13. Figure 13a–c shows three phase shifted fringe images with a phase shift of $2\pi/3$. The phase shifting is realized by spatially moving the binary structured patterns. For example, $2\pi/3$ phase shift is realized by moving the structured patterns 1/3 of the period. These fringe images can then be analyzed by the three-step phase-shifting to perform the measurement. It clearly shows that the measurement quality is very high.

Because of the nature of using binary structured patterns to generate sinusoidal fringe patterns, it allows faster image switching rate. The most recently developed DLP Discovery technology has enabled 1-bit image switching rate at tens of kHz. By applying the new fringe generation technique to this DLP Discovery projection platform, we achieved an unprecedented rate for 3D shape measurement: 667 Hz [40].

Due to the numerous advantages of using this technique to generate sinusoidal fringe patterns, it has the potential to replace the conventional fringe generation technique for 3D imaging with fringe analysis techniques.

However, this technique is not trouble free. One of the major issues is that the seemingly sinusoidal fringe pattern

is actually composed of high-frequency harmonics. This introduces measurement error. Another potential issue is the depth range; the range of high-quality fringe patterns is smaller using this technique than conventional fringe generation methods. This is because the projector cannot be defocused too little or too much for high-quality measurement. We are currently seeking hardware and software means to solve for these problems.

7 Conclusion

This paper has presented techniques for real-time 3D imaging, introducing the theory, and providing experimental results demonstrating the capabilities of each. With the Fourier analysis technique, a single fringe image can be used to reconstruct one 3D shape, although it requires surface uniformity. Essentially, this technique can reach pixel level resolution with 3D reconstruction speed equal to the frame rate of the camera. Geometry that has surface height variations or reflectivity changes with a frequency above the fringe frequency used cannot be captured with a single fringe image; in such cases, dual fringe images may be used. Using dual fringe images improves measurement accuracy, but 3D reconstruction speed is reduced to half the frame rate of the camera. Furthermore, three fringe images can be used, along with a phase-shifting technique; significantly improving accuracy, but reducing the frame rate to a third of the frame rate of the camera. With a camera that has a frame rate above 90 fps, we developed a real-time 3D imaging system that can simultaneously acquire, reconstruct, and display 3D geometry at 30 fps at a resolution of over 300,000 points per frame. Due to the very challenging nature of generating ideal sinusoidal fringe patterns, a novel approach was also discussed to significantly simplify the fringe generation, which shows great potential to be the mainstream in this field.

Acknowledgments The authors would like to thank William Lohry for his contribution on rendering the facial data with Blender, and Victor Villagomez and Ying Xu for processing the data. All these individuals are undergraduate students working under the supervision of Dr. Zhang in the 3D Machine Vision Laboratory at Iowa State University.

References

1. Baldi, A.: Phase unwrapping by region growing. Appl. Opt. **42**, 2498–2505 (2003)
2. Chyou, J.J., Chen, S.J., Chen, Y.K.: Two-dimensional phase unwrapping with a multichannel least-mean-square algorithm. Appl. Opt. **43**, 5655–5661 (2004)
3. Davis, J., Ramamoorthi, R., Rusinkiewicz, S.: Spacetime stereo: A unifying framework for depth from triangulation. IEEE Trans. Patt. Anal. Mach. Intell. **27**(2), 1–7 (2005)
4. Flynn, T.J.: Two-dimensional phase unwrapping with minimum weighted discontinuity. J. Opt. Soc. Am. A **14**, 2692–2701 (1997)
5. Geng, Z.J.: Rainbow 3D camera: new concept of high-speed three vision system. Opt. Eng. **35**, 376–383 (1996)
6. Ghiglia, D.C., Pritt, M.D.: Two-Dimensional Phase Unwrapping: Theory, Algorithms, and Software. Wiley, New York (1998)
7. Ghiglia, D.C., Romero, L.A.: Minimum l^p-norm two-dimensional phase unwrapping. J. Opt. Soc. Am. A **13**, 1–15 (1996)
8. Guan, C., Hassebrook, L.G., Lau, D.L.: Composite structured light pattern for three-dimensional video. Opt. Express **11**(5), 406–417 (2003)
9. Guo, H., Huang, P.: 3D shape measurement by use of a modified fourier transform method. In: Proceedings SPIE, vol. 7066, p. 70660E (2008)
10. Guo, H., He, H., Chen, M.: Gamma correction for digital fringe projection profilometry. Appl. Opt. **43**, 2906–2914 (2004)
11. Hornbeck, L.J.: Digital light rrocessing for high-brightness, high-resolution applications. In: Proceedings of SPIE, vol. 3013, pp. 27–40 (1997)
12. Huang, P.S., Zhang, S.: Fast three-step phase shifting algorithm. Appl. Opt. **45**, 5086–5091 (2006)
13. Huang, P.S., Hu, Q., Jin, F., Chiang, F.P.: Color-encoded digital fringe projection technique for high-speed three-dimensional surface contouring. Opt. Eng. **38**, 1065–1071 (1999)
14. Huang, P.S., Zhang, C., Chiang, F.P.: High-speed 3D shape measurement based on digital fringe projection. Opt. Eng. **42**(1), 163–168 (2002)
15. Huang, P.S., Zhang, S., Chiang, F.P.: Trapezoidal phase-shifting method for three-dimensional shape measurement. Opt. Eng. **44**, 123,601 (2005)
16. Hung, K.M., Yamada, T.: Phase unwrapping by regions using least-squares approach. Opt. Eng. **37**, 2965–2970 (1998)
17. Huntley, J.M.: Noise-immune phase unwrapping algorithm. Appl. Opt. **28**, 3268–3270 (1989)
18. Kakunai, S., Sakamoto, T., Iwata, K.: Profile measurement taken with liquid-crystal grating. Appl. Opt. **38**(13), 2824–2828 (1999)
19. Lei, S., Zhang, S.: Flexible 3-D shape measurement method using projector defocusing. Opt. Lett. **34**(20), 3080–3082 (2009)
20. Lei, S., Zhang, S.: Digital sinusoidal fringe generation: defocusing binary patterns vs focusing sinusoidal patterns. Opt. Laser Eng. **48**, 561–569 (2010)
21. Malacara, D. (ed.): Optical Shop Testing. Wiley & Sons Inc., New York (1992)
22. Merráez, M.A., Boticario, J.G., Labor, M.J., Burton, D.R.: Agglomerative clustering-based approach for two dimensional phase unwrapping. Appl. Opt. **44**, 1129–1140 (2005)
23. Pan, B., Kemao, Q., Huang, L., Asundi, A.: Phase error analysis and compensation for nonsinusoidal waveforms in phase-shifting digital fringe projection profilometry. Opt. Lett. **34**(4), 2906–2914 (2009)
24. Pan, J., Huang, P.S., Chiang, F.P.: Color phase-shifting technique for three-dimensional shape measurement. Opt. Eng. **45**(12), 013,602 (2006)
25. Radiohead: House of cards. Online: http://www.youtube.com/watch?v=8nTFjVm9sTQ (2008)
26. Rusinkiewicz, S., Hall-Holt, O., Levoy, M.: Real-time 3d model acquisition. ACM Trans. Graph. **21**(3), 438–446 (2002)
27. Salfity, M.F., Ruiz, P.D., Huntley, J.M., Graves, M.J., Cusack, R., Beauregard, D.A.: Branch cut surface placement for unwrapping of undersampled three-dimensional phase data: application to magnetic resonance imaging arterial flow mapping. Appl. Opt. **45**, 2711–2722 (2006)
28. Su, X., Zhang, Q.: Dynamic 3-D shape measurement method: a review. Opt. Laser Eng. **48**, 191–204 (2010)

29. Takeda, M., Mutoh, K.: Fourier transform profilometry for the automatic measurement of 3-D object shape. Appl. Opt. **22**, 3977–3982 (1983)
30. Zhang, L., Curless, B., Seitz, S.: Spacetime stereo: shape recovery for dynamic scenes. In: Proceedings of Computer Vison and Pattern Recognition, pp 367–374 (2003)
31. Zhang, S.: Recent progresses on real-time 3-D shape measurement using digital fringe projection techniques. Opt. Laser Eng. **48**(2), 149–158 (2010)
32. Zhang, S., Huang, P.S.: High-resolution, real-time three-dimensional shape measurement. Opt. Eng. **45**, 123,601 (2006)
33. Zhang, S., Huang, P.S.: Novel method for structured light system calibration. Opt. Eng. **45**, 083,601 (2006)
34. Zhang, S., Huang, P.S.: Phase error compensation for a three-dimensional shape measurement system based on the phase shifting method. Opt. Eng. **46**(6), 063,601 (2007)
35. Zhang, S., Yau, S.T.: High-resolution, real-time 3d absolute coordinate measurement based on a phase-shifting method. Opt. Express **14**(7), 2644–2649 (2006)
36. Zhang, S., Yau, S.T.: Generic nonsinusoidal phase error correction for three-dimensional shape measurement using a digital video projector. Appl. Opt. **46**(1), 36–43 (2007)
37. Zhang, S., Yau, S.T.: High-speed three-dimensional shape measurement using a modified two-plus-one phase-shifting algorithm. Opt. Eng. **46**(11), 113,603 (2007)
38. Zhang, S., Royer, D., Yau, S.T.: Gpu-assisted high-resolution, real-time 3-D shape measurement. Opt. Express **14**(20), 9120–9129 (2006)
39. Zhang, S., Li, X., Yau, S.T.: Multilevel quality-guided phase unwrapping algorithm for real-time three-dimensional shape reconstruction. Appl. Opt. **46**, 50–57 (2007)
40. Zhang, S., van der Weide, D., Oliver, J.: Superfast phase-shifting method for 3-D shape measurement. Opt. Express **18**(9), 9684–9689 (2010)

Author Biographies

Nikolaus Karpinsky came ISU in the fall of 2009 seeking his M.S. in Human Computer Interaction. He received his B.S. in Software Engineering from Milwaukee School of Engineering in the spring of 2009. His research interests include 3D telecommunication, augmented reality, computer vision, and human computer interaction.

Song Zhang is an assistant professor of mechanical engineering at Iowa State University. He received his doctoral degree in mechanical engineering from Stony Brook University in 2005, and worked as a post-doctor fellow at Harvard University from 2005 to 2008. His major research interests include KHz, MHz and GHz 3D imaging, biophotonic imaging, human computer interaction, and virtual reality.